ONE OF THESE POLES IS NOT LIKE THE OTHER: ASYMMETRY IN THE GLOBAL DISTRIBUTION OF LUNAR CPR ANOMALOUS CRATERS. B. J. Thomson[1], S. S. Bhiravarasu[2], C. A. Nypaver[1], G. W. Patterson[3], A. M. Stickle[3], C. I. Fassett[4], J. T. S. Cahill[3], and J. B. Plescia[5], [1]Dept. of Earth and Planetary Sciences, Univ. of Tennessee, Knoxville, TN 37996 (bthom@utk.edu), [2] Space Applications Centre (ISRO), Ahmedabad, India, [3]Planetary Exploration Group, Johns Hopkins Univ. Applied Physics Lab, Laurel, MD, [4]NASA Marshall Space Flight Center, Huntsville, AL, [5]Dept. of Geology, Univ. of Maryland, College Park, MD.

Introduction: Radar provides an ideal means to probe permanently shadowed regions on the Moon as radar provides its own illumination source. Observations from ground-based and orbital radars of the lunar polar regions, however, have yielded conflicting interpretations. Some have interpreted the returned radar polarimetric signatures as indicative of water ice [1-5], while others have asserted that the observed radar signatures could be explained by textural differences such as roughness, rather than by compositional differences [7-11]. Here we revisit the crater analysis of *Spudis et al.* [2] using an expanded set of craters [6] to explore latitudinal trends in the polarimetric signatures of impact craters.

Background: Recent analyses of the radar signatures of 6,206 craters on the lunar mare reveal systematic trends in their evolution [13]. These results indicate that the evolution of crater interiors is decoupled from their exteriors, and that all craters pass through a phase of evolution where their interiors have higher circular polarization ratio (CPR) values than their exteriors. Such craters have been termed "anomalous" [1, 2], and opposing studies have asserted that anomalous craters are either overabundant in the lunar polar regions [2, 14] or are statistically indistinguishable from their background rate of occurrence [10]. In this present work, we explore the effects of applying different thresholds or definitions of radar anomalous craters. We also examine much larger sets of craters [6, 12] to better constrain their true rate of occurrence across the Moon.

Data and Methods: In this work, we used S-band (12.6 cm wavelength, 2.38 GHz) zoom-mode swaths from Mini-RF to derive CPR, which is the ratio of the same sense of circular polarization that was transmitted (SC) to the opposite-sense circular polarization (OC) (see [15, 16] for processing details). Using a global lunar crater catalog assembled by [6] that contains 22,746 craters that range in diameter from 5–20 km, we measured CPR values using multiple definitions of CPR anomalous as described below.

There are two different definitions of CPR anomalous craters. The first definition, based on a ratio of interior and exterior values, is from [2]:

$$anom \equiv \frac{\mu_{c-int}}{\mu_{c-ext}} \geq 1.5 \qquad (1)$$

where $\mu_{\text{c-int}}$ and $\mu_{\text{c-ext}}$ are the CPR values of the crater interior and exterior, respectively. A second definition [10] of anomalous craters is based on the difference between interior and exterior values and is given in Eq. 2.

$$anom \equiv \mu_{c-int} - \mu_{c-ext} \geq 0.1 \qquad (2)$$

In addition to differing methodologies for defining CPR anomalous craters, there are also differences in the region adopted for the crater exterior. [2] took the crater exterior to be the region outside the crater rim out to a distance of two crater radii, i.e., between 1.0 and 2.0 radii. In contrast, [10] took the exterior region to be the annular zone between 1.0 and 1.414 crater radii. This particular distance ($r\sqrt{2}$) was selected so that the area of the crater exterior is equivalent to the crater interior. In the case of the larger region used by [2], the exterior annular zone has three times the area of the crater interior.

Results: Using the ratio and difference definition of CPR anomalous craters and two different assumptions about the crater exterior (i.e., out to 1.414 or 2.0 radii), there are four possible combinations as given in **Fig. 1**.

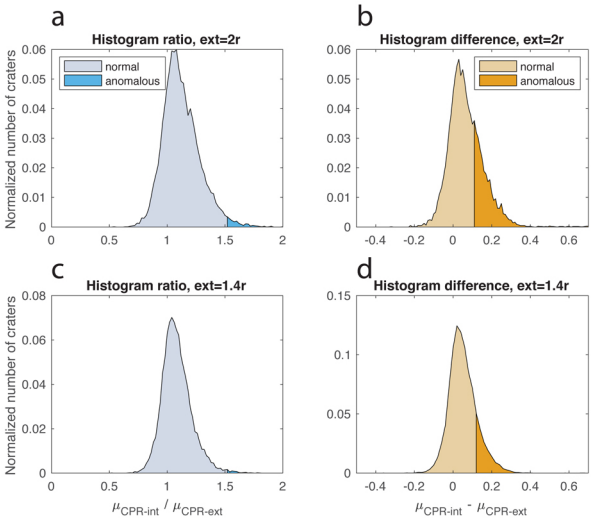

Figure 1. Histograms of lunar impact crater CPR values using different definitions of CPR anomalous. **(a)** Ratio of crater CPR interior over exterior values. Here, the exterior range is 1–2 crater radii. **(b)** Difference between crater CPR interior minus exterior values (exterior is 1–2 radii). **(c)** Ratio of crater CPR interior over exterior values. Here, the exterior range is 1.0–1.4 crater radii. **(d)** Difference between CPR interior minus exterior values (exterior is 1.0–1.4 radii).

Figs. 1a and **1c** use the ratio definition of CPR anomalous given in Eq. 1 [1, 2]; **Figs. 1b** and **1d** use the difference definition of CPR anomalous given in Eq. 2 [10]. The percentage of craters that are anomalous are 1.9% and 0.6% in **Figs. 1a** and **1c**, respectively, while the percentage of craters that are anomalous in **Figs. 1b** and **1d** are 29.3% and 18.1%, respectively. In these four cases, the percentage of craters that qualify as anomalous increases as the outer boundary of the exterior zone increases from 1.4*r* to 2.0*r*. Note that a value of 1.5 was adopted here for the CPR ratio threshold instead of the original value of 2.5 [2]; the lower value is due to a suppression of more extreme pixel values in spatial downsampling used to produce the radar mosaics [15].

Trends with Latitude: In addition to examining differences in the overall distribution of data, it is also instructive to examine trends with latitude. **Fig. 2a** gives a scatterplot of the ratio definition (Eq. 1) of CPR anomalous craters [2] as a function of lunar latitude.

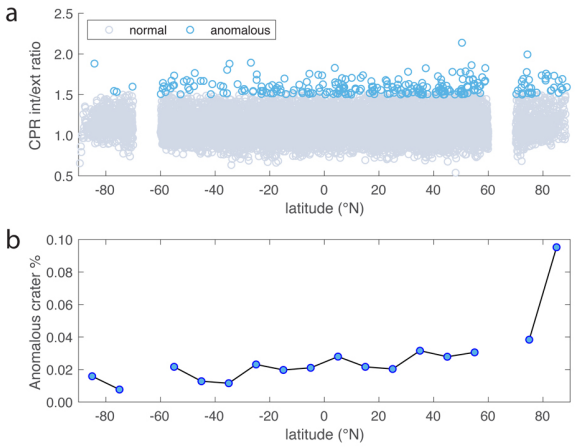

Figure 2. (a) Scatterplot of CPR interior / exterior ratio for lunar craters from [6] as a function of latitude. Craters highlighted in blue qualify as CPR anomalous after *Spudis et al.* [1, 2]. **(b)** Percentage of craters that are CPR anomalous using Eq. 1 in 10° latitude bins. Data gaps between 60–70° N and S are an artifact of processing.

A similar scatterplot using an expanded set of more than two million craters from *Robbins* [12] is given in **Fig. 3a**. Both of these plots use the more spatially expansive definition of crater exterior (i.e., out to 2 crater radii) as this region includes more of the continuous ejecta blanket [e.g., 17]. The lower panels in these two figures give the percentage of craters that qualify as anomalous in 10° latitude bins. In **Fig. 2b,** it is apparent that the north polar region >80°N has an abundance of CPR anomalous craters that approaches 10%, which is roughly three times the "background" occurrence rate of ~2–3%. In **Fig. 3b,** the percentage of craters that are anomalous in the north polar region approaches 2%, which is again three times as large as the rate of occurrence of anomalous craters in non-polar regions (here ~0.5% between 60°S to 60°N).

Discussion: The overabundance of CPR anomalous craters in the north polar region is confirmed [18, 19]. As this detection is robust using multiple definitions of CPR anomalous craters and multiple crater catalogs, this appears to be a general result, rather than a tuned result. The interesting dichotomy between the north and south polar regions remains to be explored. While both polar regions exhibit average radar backscatter properties typical for the highland areas of the Moon [e.g., 7, 15], the south polar region is dominated by the rim of the South-Polar Aiken basin, and the more rugged topography may slightly disfavor prolonged ice stability.

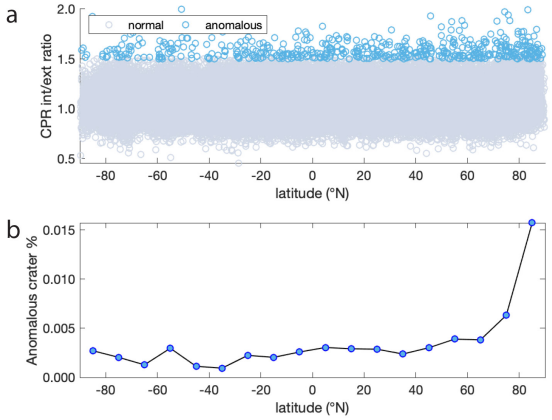

Figure 3. (a) Scatterplot of CPR interior / exterior ratio for lunar craters from [12] as a function of latitude. Craters highlighted in blue qualify as CPR anomalous after [1, 2]. **(b)** % of craters that are CPR anomalous in 10° latitude bins.

Acknowledgments: This work was supported in part by grants from NASA LDAP and a grant from JHU/APL through the NASA LRO mission.

References: [1] Spudis P.D. et al. (2010) *GRL*, *37*, L06204. [2] Spudis P.D. et al. (2013) *JGR*, *118*, 2016-2029. [3] Thomson B.J. et al. (2012) *GRL*, *39*, 14201. [4] Nozette S. et al. (1996) *Science*, *274*, 1495-1498. [5] Patterson G.W. et al. (2017) *Icarus*, *283*, 2-19. [6] Povilaitis R. et al. (2018) *PSS*, *162*, 41-51. [7] Campbell D.B. et al. (2006) *Nature*, *443*, 835-837. [8] Stacy N.J.S. et al. (1997) *Science*, *276*, 1527-1530. [9] Fa W. & Cai Y. (2013) *JGR*, *118*, 1582-1608. [10] Fa W. & Eke V.R. (2018) *JGR*, *123*, 2119-2137. [11] Eke V.R. et al. (2014) *Icarus*, *241*, 66-78. [12] Robbins S.J. (2019) *JGR*, *124*, 871. [13] Fassett C.I. et al. (2018) *JGR*, *123*, 3133-3143. [14] Thomson B.J. et al. (2012) *LPSC*, abstract #2104. [15] Cahill J.T.S. et al. (2014) *Icarus*, *243*, 173-190. [16] Carter L.M. et al. (2017) *IEEE Trans. Geosci. Rem. Sen.*, *55*, 1915-1927. [17] Neish C.D. et al. (2013) *JGR*, *118*, 2247-2261. [18] Thomson B.J. et al. (2019) *LPSC*, Abstract #2855. [19] Thomson B.J. et al. (2020) *LPSC*, abstract #2424.